Ferromagnetic resonance force microscopy of individual domain wall

A. Volodin, C. Van Haesendonck, E. V. Skorokhodov, R. V. Gorev, and V. L. Mironov

Citation: Appl. Phys. Lett. **113**, 122407 (2018); doi: 10.1063/1.5040072
View online: https://doi.org/10.1063/1.5040072
View Table of Contents: http://aip.scitation.org/toc/apl/113/12
Published by the American Institute of Physics

Ferromagnetic resonance force microscopy of individual domain wall

A. Volodin,[1,a)] C. Van Haesendonck,[1] E. V. Skorokhodov,[2] R. V. Gorev,[2] and V. L. Mironov[2]
[1]*KU Leuven, Afdeling Vaste-stoffysica en Magnetisme, Celestijnenlaan 200D, BE-3001 Leuven, Belgium*
[2]*Institute for Physics of Microstructures RAS, GSP-105, Nizhny Novgorod 603950, Russia*

(Received 14 May 2018; accepted 8 September 2018; published online 21 September 2018)

We report on ferromagnetic resonance force microscopy (FMRFM) based investigations of the ferromagnetic resonance of a single domain wall (DW) in a V-shaped planar permalloy nanowire (NW) which is bent by 60°. A pronounced resonance associated with the DW is observed at 1.6 GHz. FMRFM imaging at the resonance frequency confirms the localization of the resonant mode in the DW area. The measured spectra and spatial distribution of the resonant signal are in good agreement with the results of micromagnetic modeling. *Published by AIP Publishing.*
https://doi.org/10.1063/1.5040072

Magnetic domain walls (DWs) are spatially localized inhomogeneous features of magnetization in ferromagnetic structures that constitute a main ingredient in emerging spintronic applications, including magnetic data storage and processing systems,[1] elements of magnetic logics,[2,3] and devices for the manipulation of magnetic microbeads used in biotechnology.[4] Resonant DW excitations may be applied in magnonic devices.[5] The ability to exploit dynamic and resonant phenomena of DWs in applications requires detailed investigations of these phenomena. One of the most effective methods for investigating the dynamic and resonant properties of DWs is ferromagnetic resonance (FMR) spectroscopy.[6] However, the FMR measurements in standard spin-resonance spectrometers are limited only to samples containing large numbers of DWs, with inevitable distribution related averaging effects. As a result, FMR properties of individual DWs remain inaccessible although it is very important to obtain information at the individual DW level. A variety of spatially resolved measurement techniques for the investigation of FMR have been developed, including microscopy based on Brillouin light scattering,[7] time-resolved magneto-optical Kerr microscopy (TR-MOKE),[8] X-ray magnetic circular dichroism,[9] scanning thermal microscopy (SThM),[10] near-field microwave microscopy (SMM),[11] and ferromagnetic force resonance microscopy (FMRFM).[12] Scanning probe magnetometry using nitrogen vacancy centers in diamond (NV-SPM)[13] has recently been added to these techniques. Each of these techniques has its own advantages and disadvantages when it comes primarily to detection sensitivity and spatial resolution. The emerging NV-SPM technique apparently has the greatest advantages among the indicated techniques, but its realization requires sophisticated equipment. The lateral resolution of the optical techniques such as TR-MOKE is restricted by the limited focusing of the exciting laser beam. The spatial resolution of SThM and SMM is relatively high and is limited by the size of the probe, but the detection sensitivity of both techniques is low. An approach with very high sensitivity for locally detecting FMR is offered by FMRFM, which is one of the up-to-date extensions of scanning force microscopy. FMRFM allows measuring the FMR spectra of individual submicron size magnets.[14] While exhibiting an exceptional sensitivity, FMRFM is restricted in its spatial resolution to at best a few 100 nm, due to the long range of the probe stray field. Another important advantage is that FMRFM is the only technique that can detect the dynamics of the longitudinal magnetization component.[15] We also note that the spatially confined magnetic field of the probe can be used to localize the FMR mode[16] and thus improve the spatial resolution.

Recently, time-resolved Kerr microscopy was applied for investigating the eigenmodes of individual DWs in ferromagnetic nanowires (NWs).[17] In this letter, we report on the FMRFM based observation of FMR of individual DWs that emerge in bent planar permalloy NWs. The FMR spectroscopy results and the measured distribution of the magnetization oscillations are compared with the results of micromagnetic modeling.

The magnetic permalloy V-shaped NWs bent by 60° (with shoulders having a length of 3000 nm and a width of 600 nm) are fabricated on 100 μm thick glass substrates and are ordered in rectangular arrays containing 10×2 NWs with 11 μm spacing. The NW samples are defined by e-beam lithography with metallization and lift-off of a 30 nm thick $Ni_{80}Fe_{20}$ layer deposited using dc-magnetron sputtering.[18] A scanning electron microscopy (SEM) micrograph of a V-shaped NW is shown in Fig. 1(a). In these NWs, DWs can be easily induced by an external magnetic field. The spatial separation of the NWs by 11 μm

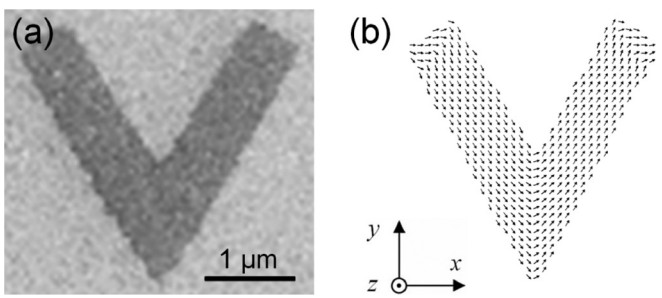

FIG. 1. (a) SEM image of a $Ni_{80}Fe_{20}$ V-shaped nanowire (NW). (b) Simulated distribution of the magnetization in the NW after magnetizing the NW in the *x*-direction.

a)Author to whom correspondence should be addressed: Alexander.Volodin@kuleuven.be

avoids cross coupling and ensures an "individual" NW structure approach for the FMRFM experiments.

The magnetic states and FMR modes in the NWs have been modeled using the Object Oriented Micro Magnetic Framework (OOMMF) simulator[19] based on numerical solution of the Landau–Lifshitz–Gilbert equation[20] for the magnetization of the sample. The calculations are carried out for the following permalloy parameters: the magnetization in saturation is 8×10^5 A/m, the exchange stiffness is 8.4×10^{-12} J/m, and the dissipation constant is 0.01. The computational cell has a size of $10 \times 10 \times 30\,\text{nm}^3$.

To detect the resonance response of DW, we exploit the local selectivity and high sensitivity of FMRFM. Our FMRFM setup is based on a customized AFM1[21] setup with a fiber optical interferometer (attocube). A nearly spherical Co probe with a diameter of $\sim 7\,\mu$m is attached to the end of a tipless cantilever (TL-CONT from NANOSENSORS) with a force constant of ~ 0.1 N/m and is used to localize the region where FMR is excited by a microwave strip-line inductor. Within this region, the sum of the internal magnetic field and the probe magnetic field determines the field for the resonance condition of the DW. The field gradient produced by the probe couples the modulated high-frequency magnetization component to the cantilever that serves as a resonant (at the modulation frequency) micromechanical force detector. The high quality factor ($\sim 5 \times 10^3$ in vacuum) of the mechanical resonator provides its unique sensitivity. The magnetization in the NWs is manipulated using 100% amplitude modulation of the microwave field at the cantilever resonance frequency of ~ 15.3 kHz while sweeping the microwave frequency in the range of 0.1–3 GHz. The measurements are performed at room temperature.

The Neel type "head-to-tail" DW configuration [Fig. 1(b)] is induced by applying a magnetic field of 500 Oe in the x-direction to saturate the NW magnetization and subsequently decreasing the field to zero. When performing the FMRFM measurements, an in-plane magnetic field of 50 Oe is applied in the x-direction to stabilize this DW state.

Because the probe generates a sufficiently strong field, measures need to be taken to minimize its disturbance of the DW. In order to avoid possible destruction of the DW by the probing field, we magnetize the probe in a 1 T field tilted by an angle of $\sim 30^\circ$ from the direction perpendicular to the sample. This inclination creates a probe induced field component directed along the x-axis when the probe is positioned above the DW, which has a stabilizing effect on the DW. To evaluate the effective magnetic moment of the probe after magnetization, we rely on mechanical magnetometry[22] based on monitoring of the mechanical resonance frequency of the cantilever scanned above a current-carrying microfabricated ring[23] with an inner diameter of 5 μm. The magnetic moment of the probe is estimated to be $\sim 3 \times 10^{-8}$ emu. The accuracy of this evaluation is estimated to be around 20%.

The stray field of the probe introduces an additional inhomogeneous external magnetic field at the NW that critically depends on the probe-sample separation. In close proximity to the NW, this field can modify or even destroy the DW. We use relatively large separation values in the micrometer range to ensure that this field is weak compared to the internal fields of the NW structure. The typical FMRFM spectra acquired at slightly different probe-sample separations in the range of 3.4–2.0 μm are presented in Fig. 2(a). Each of the FMRFM spectra in the frequency range of 0.5 to 2.5 GHz consists of a single resonance peak. The spectra are obtained with a microwave magnetic excitation field applied along the y-axis [see the axis configuration in Fig. 1(b)]. It should be noted that almost all measurements are carried out using these excitation conditions. An example of one of the spectra acquired using a microwave field directed along the x-axis is presented in Fig. 2(a) for comparison. The spectra obtained for an excitation field applied along the y-axis are ~ 7 times more intensive than for excitation along the x-axis. We explain this observation by considering the fact that the magnetization distribution in the DW has a preferred direction along the x-axis. Therefore, applying a microwave magnetic field along the y-axis leads to a more efficient excitation of the resonance.

The resonance peak shifts to higher frequency values, and its intensity increases as the probe approaches the sample surface [Fig. 2(a)]. The observed shifts of the spectra can be explained by the effect of the in-plane component of the magnetic field generated by the probe. Similar displacements of the spectra were observed when a small magnetic field is applied along the x-axis. From such measurements, we are able to estimate the field component increase induced by the probe as 46 ± 5 Oe when the probe-NW spacing decreases from 3.3 μm to 2.0 μm [Fig. 2(a)].

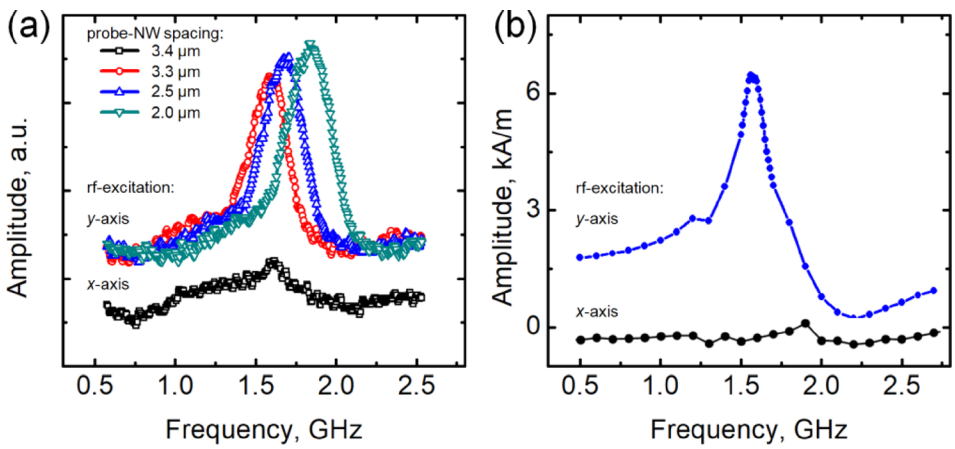

FIG. 2. (a) FMRFM spectra measured at $H = 50$ Oe aligned along the film plane perpendicular to the DW for various probe-sample separations and for two orientations of the microwave magnetic field excitation, i.e., directed along the y-axis (upper curves) and along the x-axis (lower curve). The spectra have been vertically offset. (b) Modeled DW FMR spectra obtained at a magnetic field of 50 Oe aligned along the x-axis in the film plane. The upper and lower curves represent the spectra obtained for the excitation magnetic fields applied along the y-axis and the x-axis, respectively.

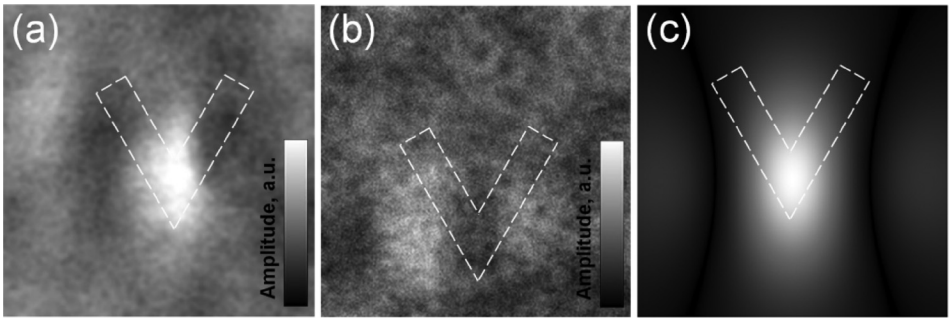

FIG. 3. (a) $6 \times 6\ \mu m^2$ FMRFM images acquired at the DW resonant microwave frequency of 1.6 GHz and (b) at a frequency corresponding to a detuning by 250 MHz. The probe-NW separation is 3.3 μm. (c) Spatial distribution of the simulated amplitudes of the FMRFM signal at a height of 3.3 μm from the surface.

The variation of the intensity of FMRFM spectra with the probe-sample separation in the indicated range may be explained in a straightforward way by the fact that the probe field gradient increases with the decreasing distance, resulting in an increase in the FMRFM signal. When the probe approaches the surface of the sample at distances $<2\ \mu$m, the influence of the magnetic field of the probe increases substantially. This results in dramatic disturbances of the measured spectra. In view of the complexity of the observed changes in the spectra, we do not analyze these changes in this paper. A detailed analysis can be carried out by taking into account localization of the resonance modes of the DW for the used specific geometry of the orthogonal magnetic fields of the probe and the NWs.[24]

In Fig. 3(a), we present a typical result for a FMRFM lateral scan acquired at 1.6 GHz across a NW. This frequency excites the resonance of the DW when the probe is located above the center of the DW. By decreasing the frequency by ~250 MHz [see Fig. 3(b)], the total magnetic field experienced by the DW when the probe is located above the center of the DW exceeds the resonance field and thus the signal is reduced. Moving away from the center of the DW reduces the total magnetic field experienced by the DW and increases the signal as the peak of the FMR spectrum is approached. The resonant conditions then appear as a halo in the FMRFM image.[25]

In a typical FMRFM experimental configuration, the probe magnetization is parallel to the normal field component of the thin-film magnetic microstructures. In addition, the external applied field is also directed along the normal.[26] In our specific case, the investigated DWs have in-plane magnetization vectors. Since the magnetization vectors of the DWs are arranged in-plane, the question arises as to how the probe with a large perpendicular magnetization component couples to a DW. The force and torque are the two components producing a deformation of the cantilever in the z-direction.[27] The DW dipolar field contributes to the torque. The force acting on the probe results from the gradient of the x-component of the probe magnetic moment. The presence of these two components of the probe−DW interaction can account for the coupling of the probe to a DW.

In order to analyze the FMR of a DW, we have simulated the time dependences of the steady-state oscillations induced by the microwave magnetic field (with amplitude of 1 Oe) for all magnetization components. The simulations are performed for an alternating magnetic field directed along the x-axis and along the y-axis. The results of our micromagnetic simulations of the magnetization oscillation spectrum in the frequency range of 0.1–5 GHz are presented in Fig. 2(b). The intense peak at 1.6 GHz is related to the resonance, which corresponds to the localized mode of the DW oscillations excited by the alternating magnetic field directed along the y-axis. Note that the main (quasi-uniform) FMR mode excited in the NWs corresponds to a frequency of ~7 GHz, which is well above the main mode resonant frequency of the DWs. The simulated DW mode spectrum shown in Fig. 2(b) fits well to the measured spectrum of the NWs with the FMRFM probe localized above a DW [see Fig. 2(a)]. On the other hand, upon the application of an alternating magnetic field along the x-axis, this peak disappears [lower curve in Fig. 2(b)]. The very pronounced decrease in the intensity of the peak in the spectrum measured under this condition of excitation [see Fig. 2(a)] is consistent with our model based simulation.

In order to model the FMRFM images, we have calculated the spatial distributions of the z-gradient of the x-component of the alternating magnetic field generated by the sample magnetization in the scanning plane of the probe arranged at a height of 600 nm. We expected that the probe couples to the x-component of the NW local magnetization. The modeled spatial distribution of the FMRFM signal amplitude, which is presented in Fig. 3(c), is in many respects similar to the contrast of the FMRFM image obtained experimentally at the resonant microwave frequency [see Fig. 3(a)]. The spectral features associated with resonances in proximity to the probe provide FMRFM images [Figs. 3(a) and 3(b)] of a permalloy microstructure in which the individual DW is clearly resolved. The difference in the spectra in Fig. 2(a) for different relative orientations of the exciting field and the DW also indicates that the resonance belongs to the observed DW. These two pieces of evidence and an agreement between the experimental and simulated results strongly suggest that the dynamic oscillation mode we observe is due to the dynamics of the DW and not to some other ferromagnetic resonance or spin-wave phenomenon.

In summary, we have probed the FMR properties of bent planar permalloy NWs containing a localized DW using FMRFM. We have demonstrated that the FMRFM technique provides the possibility to observe and investigate the dynamic properties of an individual DW.

The authors are thankful to A. A. Fraerman for valuable discussions. The sample preparation and micromagnetic simulations were supported by the Russian Science Foundation (Project No. 16-12-10254).

[1]S. S. P. Parkin, M. Hayashi, and L. Thomas, Science **320**, 190 (2008).
[2]M. Hayashi, L. Thomas, R. Moriya, C. Rettner, and S. S. P. Parkin, Science **320**, 209 (2008).
[3]M. Haraa, J. Shibata, T. Kimura, and Y. Otani, Appl. Phys. Lett. **89**, 192504 (2006).
[4]E. Rapoport, D. Montana, and G. S. D. Beach, Lab Chip **12**, 4433 (2012).
[5]S. J. Hermsdoerfer, H. Schultheiss, C. Rausch, S. Schäfer, B. Leven, S.-K. Kim, and B. Hillebrands, Appl. Phys. Lett. **94**, 223510 (2009).
[6]M. Bailleul, R. Höllinger, K. Perzlmaier, and C. Fermon, Phys. Rev. B **76**, 224401 (2007).
[7]S. Demokritov, B. Hillebrands, and A. N. Slavin, Phys. Rep. **348**, 441 (2001).
[8]B. L. Petersen, A. Bauer, G. Meyer, T. Crecelius, and G. Kaindel, Appl. Phys. Lett. **73**, 538 (1998).
[9]D. A. Arena, E. Vescovo, C.-C. Kao, Y. Guan, and W. E. Bailey, J. Appl. Phys. **101**, 09C109 (2007).
[10]R. Meckenstock, Rev. Sci. Instrum. **79**, 041101 (2008).
[11]C. H. Joseph, G. M. Sardi, S. S. Tuca, G. Gramse, A. Lucibello, E. Proietti, F. Kienberger, and R. Marcelli, J. Magn. Magn. Mater. **420**, 62 (2016).
[12]Z. Zhang, P. C. Hammel, and P. E. Wigen, Appl. Phys. Lett. **68**, 2005 (1996).
[13]F. Casola, T. van der Sar, and A. Yacoby, Nat. Rev. Mater. **3**, 17088 (2018).
[14]G. de Loubens, V. V. Naletov, O. Klein, J. Ben Youssef, F. Boust, and N. Vukadinovic, Phys. Rev. Lett. **98**, 127601 (2007).
[15]O. Klein, V. Charbois, V. V. Naletov, and C. Fermon, Phys. Rev. B **67**, 220407 (2003).
[16]I. Lee, Y. Obukhov, G. Xiang, A. Hauser, F. Yang, P. Banerjee, D. V. Pelekhov, and P. C. Hammel, Nature **466**, 845 (2010).
[17]A. T. Galkiewicz, L. O'Brien, P. S. Keatley, R. P. Cowburn, and P. A. Crowell, Phys. Rev. B **90**, 024420 (2014).
[18]E. V. Skorohodov, R. V. Gorev, R. R. Yakubov, E. S. Demidov, Y. V. Khivintsev, Y. A. Filimonov, and V. L. Mironov, J. Magn. Magn. Mater. **424**, 118 (2017).
[19]M. J. Donahue and D. G. Porter, NISTIR Interagency Report No. 6376 (National Institute of Standards and Technology, Gaithersburg, 1999).
[20]W. F. Brown, Jr., *Micromagnetics* (John Wiley, New York, 1963), p. 143.
[21]See http://www.attocube.com/attomicroscopy/state-art-systems/attoafmi/ for a description of the AFM1 system.
[22]H. Lavenant, V. Naletov, O. Klein, G. de Loubens, L. Casado, and J.-M. De Teresa, Nanofabrication **1**, 65 (2014).
[23]L. Kong and S. Y. Chou, Appl. Phys. Lett. **70**, 2043 (1997).
[24]E. V. Skorohodov, M. V. Sapozhnikov, and V. L. Mironov, Tech. Phys. Lett. **44**, 203 (2018).
[25]T. Mewes, J. Kim, D. V. Pelekhov, G. N. Kakazei, P. E. Wigen, S. Batra, and P. C. Hammel, Phys. Rev. B **74**, 144424 (2006).
[26]P. E. Wigen, M. L. Roukes, and P. C. Hammel, "Ferromagnetic resonance force microscopy," in *Spin Dynamics in Confined Magnetic Structures III, Topics in Applied Physics*, edited by B. Hillebrands and A. Thiaville (Springer-Verlag, Berlin, Heidelberg, 2006), Vol. 101, pp. 105–136.
[27]O. Klein and V. V. Naletov, C. R. Phys. **5**, 325 (2004).